Progress In Electromagnetics Research M, Vol. 71, 179–188, 2018

Capacitor-Inductor-Loaded, Small-Sized Loop Antenna for WLAN Notebook Computers

Saou-Wen Su*

Abstract—A small-sized loop antenna loaded with the series-connected capacitor and inductor for wireless local area network (WLAN) operation is proposed. The main radiator of an L-shaped, loop structure and its small ground were constructed on a single-layered FR4 substrate of thickness 0.8 mm and occupied a miniature size of 5 mm × 20 mm only. It was found that by loading the series-connected capacitor and inductor between the antenna feed port and the loop radiator, the quarter-wavelength loop resonance can be easily excited together with the controllable half-wavelength resonance. The design prototype was able to operate in the 2.4-GHz (2400–2484 MHz) and 5.8-GHz (5725–5825 MHz) WLAN bands. The proposed antenna was simple in structure and yet provided dual-band operation and good radiation performance.

1. INTRODUCTION

Notebook computers have been favored by the end users in various fields because of their great mobility and computing power. In the designs of the notebook computers, the antenna plays an important role regarding to stable wireless connection. For wireless local area network (WLAN) notebook antenna designs, the antennas are popularly placed along the top edge of the supporting metal frame of the display [1–15] owing to providing better wireless coverage and being away from the system-level noise. Many promising antennas for notebook computer applications, including the short-circuited monopole and planar inverted-F antennas (PIFAs) [1–9], coupled-fed monopole and PIFAs [10–12], slot antennas [13–15], etc. have been reported in the literature. These designs require either a lateral length larger than 30 mm or an antenna height larger than 5 mm. To accommodate more antennas in limited space for higher data rate, for example 4×4 WLAN antennas, the lateral size reduction in the notebook antennas is much in demand. In addition, for the present-day, large screen-to-body-ratio notebooks, the narrow bezel between the edge of the display and the outside border of the casing can be as small as 5 mm. To meet these requests, a new, small-sized antenna having the overall area of 5 mm × 20 mm only is proposed in this paper.

The antenna type used in this study is of loop antennas, which are substantially different from those notebook antennas studied in [1–15]. Loop and folded loop antennas have been favorable to applications in WLAN access points [16–22] and mobile phones [23–27] owing to their self-balanced structure of one-wavelength loops [16–22] and offering multi-resonant modes [23–26]. These loop antennas mainly operate at their half-, one-, and one-half-wavelength resonant modes, which make them larger than those quarter-wavelength antennas [1–12] and can not meet the size requirement as mentioned. For smaller loops, the loop antennas operating at the quarter-wavelength resonant mode [27, 28] were presented. Although the loop size can be minimized, the printed matching circuit in [27] and the dual-loop structure

Received 19 June 2018, Accepted 1 August 2018, Scheduled 10 August 2018

* Corresponding author: Saou-Wen Su (Saou-Wen_Su@asus.com).
The author is with the Antenna Design Department, Advanced EM & Wireless Communication R&D Center ASUS, Taipei 11259, Taiwan.

with the on-boarding matching circuit in [28] are rather complicated. These designs are still for mobile-phone applications, and to the authors' knowledge, very scant loop antennas have been applied to the notebook computers. Quite recently, a compact and printed loop antenna design was proposed for notebook applications [29]. The design utilized a capacitively-driven feed around the feed port and a chip inductor at the loop end together with a tiny cut in the antenna ground. Despite the loop operates at its quarter- and half-wavelength modes for the 2.4 and 5.2/5.8-GHz WLAN bands, the antenna configuration and parameters thereof are complicated.

The proposed antenna was very simple in structure and comprised an L-shaped loop radiator and a small antenna ground. The length of the L-shaped loop was about 16.3 mm (about 0.13-wavelengths in free space at 2445 MHz), and fed in the corner of the substrate and short-circuited opposite the antenna feed port in the diagonal corner. The small antenna ground was reserved in the design footprint for grounding the cable. The cable is usually not allowed to be routed behind the display owing to the concern for the back pressure on the display. Between the feed port and the loop radiator, a series-connected matching circuit consisting of one capacitor and one inductor was loaded. The series capacitor, similar to the coupling gap in [28, 29], helped the loop generate the quarter-wavelength resonant mode. By further inserting the chip inductor in series with the capacitor, the loop's half-wavelength resonant mode can be easily adjusted without affecting the quarter-wavelength loop mode. The proposed antenna was first analyzed in the simulation and validated by measurement.

2. PROPOSED SMALL-SIZED LOOP ANTENNA

2.1. Antenna Configuration

Figure 1(a) illustrates the proposed loop antenna placed above the top edge of the supporting metal frame of the notebook computer display for prototype studies. The design was formed on a 0.8-mm-thick, flame retardant 4 (FR4) dielectric substrate ($\varepsilon_r = 4.4$) of size 5 mm × 20 mm and comprised an L-shaped loop radiator and a small antenna ground. The metal frame of a 14-inch display measuring 2.2 mm × 182 mm × 315 mm was treated as the large system ground for both the antenna and the electromagnetic interference (EMI) grounding. The antenna was spaced 40 mm apart from the right side. This 40 mm clearance area is usually reserved for the mechanical structures and not available for antenna placement. Notice that the size of the large ground plane as the display metal frame was selected as a design example for practical applications not for limiting the proposed design.

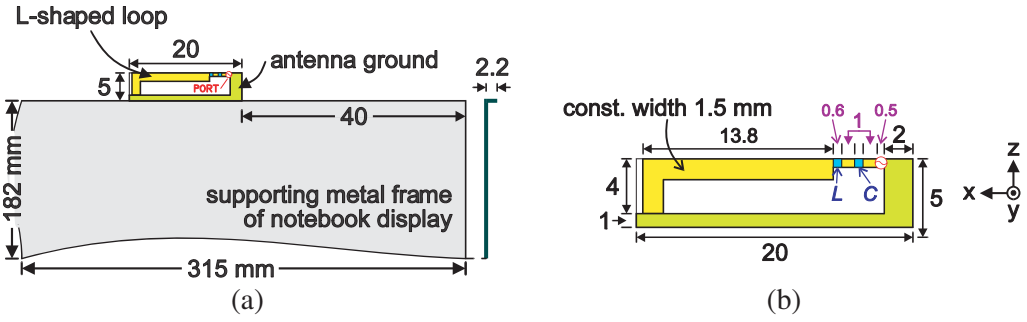

Figure 1. (a) Configuration of the proposed, printed loop antenna affixed to the supporting metal frame of a notebook display. (b) Detailed dimensions of the loop antenna.

The L-shaped loop and its ground plane formed a compact rectangular structure. The antenna feed port was arranged in the corner of the substrate about 5 mm above the display metal frame. This arrangement can be required by some cases that the antenna feeding cable needs to be routed along the top edge of the notebook cover therein or above the camera module. Fig. 1(b) details the parameters of the prototype The loop radiator occupied an area of 4 mm × 13.8 mm only and had a constant strip width of 1.5 mm. The small antenna ground comprised one horizontal and one vertical portion. For practical applications, the copper tape was used to connect the antenna ground to the display metal

frame, and thus, the horizontal ground portion was reserved in the design footprint. For testing the antenna, a 50-Ω mini-coaxial cable of length 50 mm was used to feed the loop across a tiny feed gap of 0.5 mm. In this case, the vertical ground provided the grounding area for the outer shielding of the feeding cable.

Between the antenna feed port and the loop radiator, a series-connected circuit consisting of two lumped elements was inserted. One capacitor and one inductor of Murata 0402 form factor were employed and occupied a tiny footprint of size 0.6 mm × 3.2 mm. By carefully tuning the capacitor and inductor values, dual-band WLAN operation can be achieved. The length of the L-shaped loop for the designed lower and the upper bands corresponded to about 0.13- and 0.31-wavelengths in free space respectively. However, by considering the effects of the effective dielectric constant of the substrate (ε_{eff} about 3.32 here) for the antenna as a transmission line [30], the resonant length of the loop would be closer to the quarter- and the half-wavelengths at the center frequency of the lower and the upper bands. The near optimum parameters in this study were obtained using the electromagnetic solver, ANSYS HFSS [31].

2.2. Controlling Mechanisms

To better understand the proposed antenna, a simple, half-wavelength loop antenna (see Ant1 in Fig. 2) was studied. The simulated return loss and the input impedance for the simple loop antenna are shown in Fig. 2; the dimensions are kept the same as those in Fig. 1 except for the loop length altered from 13.8 to 17 mm. It is seen that a single resonance at 5860 MHz is generated. This resonance represents the fundamental resonant mode of the typical, half-wavelength loop antenna. Over the 1–4-GHz lower band [see Fig. 2(b)], very large inductance of about 2430 Ω and resistance of about 140 Ω with the anti-resonance at 2.75 GHz are observed, making Ant1 non-responsive in the desired 2.4 GHz band.

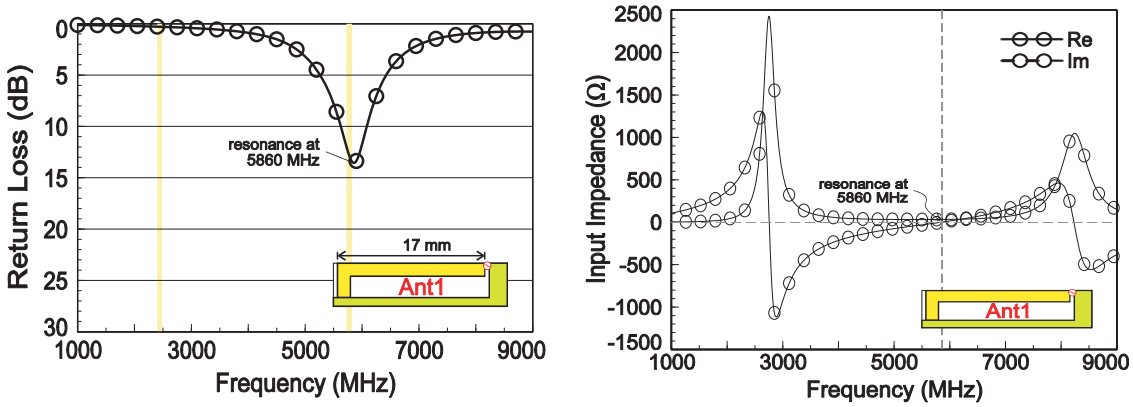

Figure 2. Simulated (a) return loss and (b) input impedance for the simple loop (Ant1, proposed without series-connected capacitor and inductor).

Figures 3(a), (b) show the simulated return loss and the input impedance for the simple loop antenna loaded with one capacitor only. The loop length is 15.4 mm [see Ant2 in Fig. 3(a)] and other dimensions remain the same as shown in Fig. 1. Over the lower and the upper bands are the two resonant modes excited. The half-wavelength loop mode of Ant2 shifts toward the higher frequencies from 5860 to 7135 MHz owing to the smaller loop length of Ant2 compared with that of Ant1. In Fig. 3(b), the inductive reactance in the lower band becomes much smaller, compared with that for Ant1 in Fig. 2(b), such that the zero reactance can be achieved. The frequency of the anti-resonance also moves to about 3 GHz with reduced resistance from about 2430 to 1200 Ω. These properties allow Ant2 to generate the quarter-wavelength loop resonance in the lower band. The two input-impedance curves for Ant1 and Ant2 on the Smith chart in the frequency range of 2–3 GHz are shown in Fig. 3(c). For Ant1, the impedance at 2505 MHz shows very large resistance toward the open-circuit point on the

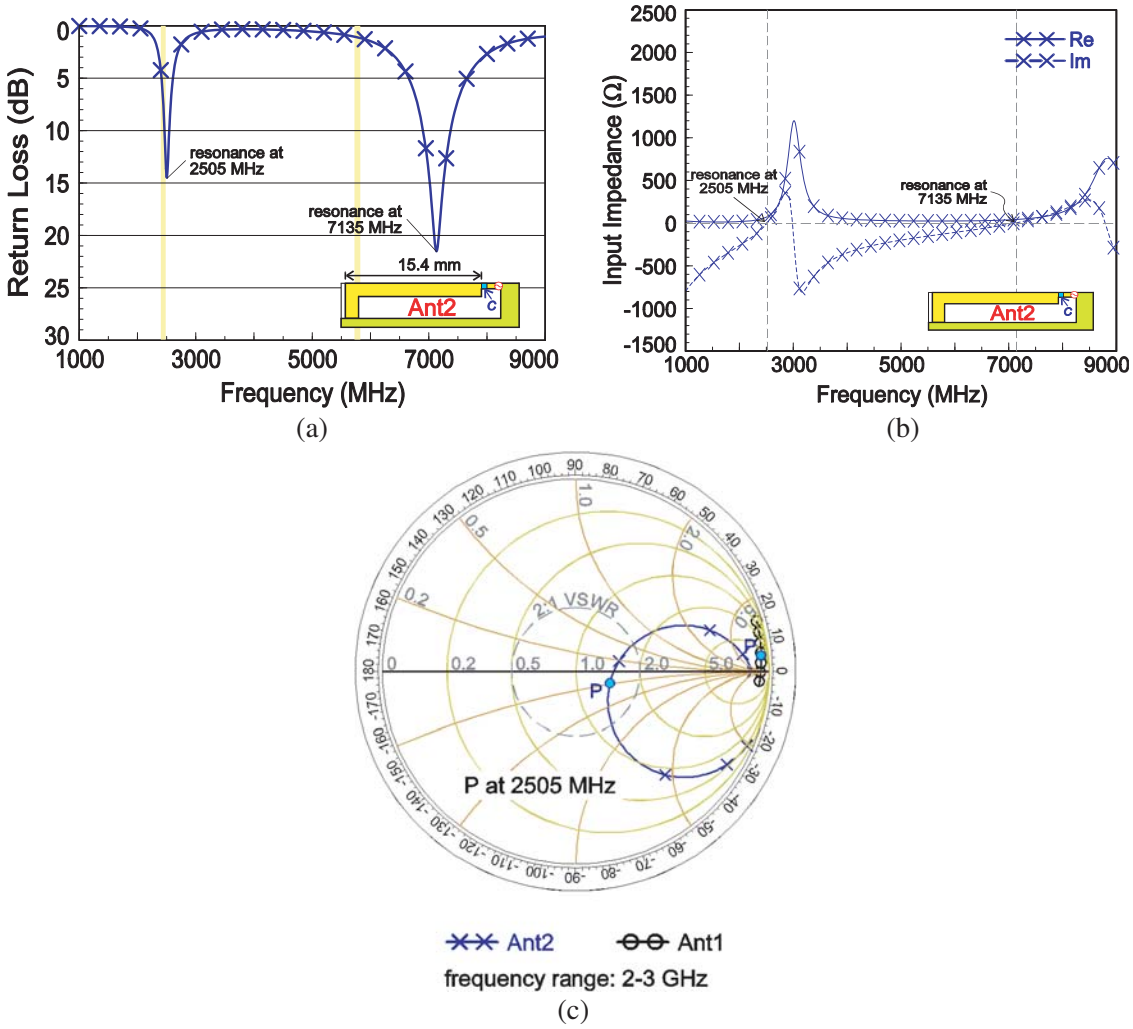

Figure 3. Simulated (a) return loss, (b) input impedance for the loop with the capacitor only (Ant2, proposed without inductor; $C = 0.1$ pF), (c) input impedance on the Smith chart for Ant2 and Ant1 in the 2–3 GHz frequency range.

Smith chart and is located in the large inductance locus, which confirms the non-responsive resonance over that 2–3-GHz band. For Ant2, with the aid of the loaded capacitor, the large inductance can be compensated. At the same time, the phase of the frequency point at 2505 MHz moves counterclockwise toward the center 50 Ω point on the chart, making it possible for Ant2 to generate additional loop mode in the lower band.

The value of the capacitor is a determining factor as to how well matched the lower-band impedance. Because the impedance curves and anti-resonance frequency in the lower band are much affected by the capacitor C, this property effects the change in the slope of impedance curves in the upper band. In this case, the operating frequencies of the upper band are also affected. Fig. 4 shows the simulated return loss as a function of the capacitor C for Ant2. It can be seen that the smaller values of the capacitor C lead to higher frequencies and better impedance matching over the lower and upper bands. The resistance also becomes smaller to be close to 50 Ω level (for brevity, input impedance not given). Because the smallest capacitance available is 0.1 pF (Murata GJM15 series used here), it is not practical to simulate an even smaller capacitor value in the study. To further decrease the upper-band frequencies to the desired WLAN band, the inductor is introduced in series with the capacitor between the capacitor and the loop radiator.

The results of the simulated return loss and the input impedance for the loop loaded with the

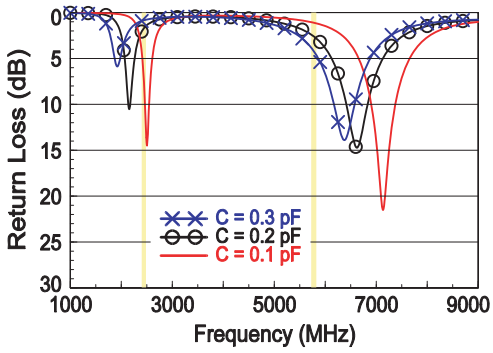

Figure 4. Simulated return loss for Ant2 studied in Fig. 3 as a function of the capacitor C.

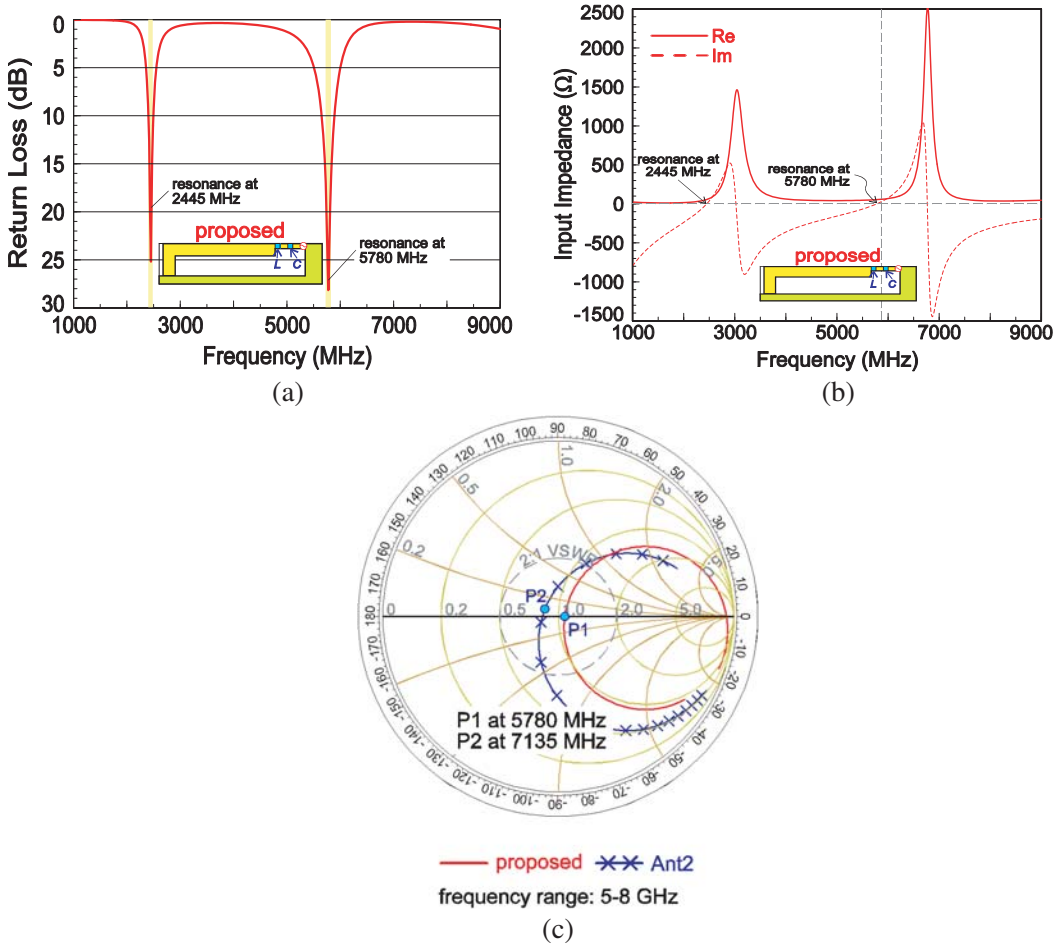

Figure 5. Simulated (a) return loss, (b) input impedance for the loop antenna loaded with the series-connected capacitor and inductor; $C = 0.1$ pF, $L = 4.8$ nH, (c) input impedance on the Smith chart for proposed and Ant2 in the 5–8-GHz frequency range.

series-connected capacitor and inductor are presented in Fig. 5. In Fig. 5(a), the two resonances with good impedance matching at 2445 and 5780 MHz for the 2.4 and 5.8 GHz bands are obtained. The characteristics of the input impedance over the 1–4-GHz lower band are similar between the proposed and Ant2 [see Fig. 5(b) and Fig. 3(b)]. For the proposed design, the zero-reactance frequency point slightly shifts toward the lower frequencies from 2505 to 2445 MHz with reduced resistance from 72 to

55 Ω. For upper band operation, the half-wavelength loop mode moves from 7135 MHz (Ant2 at P2) to 5780 MHz (proposed at P1) [also see Fig. 5(c)]. The inductor changes the upper-band frequencies rather than the impedance matching of the loop therein.

The inductor in this design acted like a low-pass matching circuit and mainly determined the operating frequencies of the half-wavelength loop mode. Fig. 6 shows the simulated return loss as a function of the inductor L for the proposed loop. It is quite straightforward to see that with an increase in the inductor value, the antenna frequencies decrease over the upper band while the lower-band frequencies are nearly the same. This result again confirms the phenomenon in Fig. 5(a) and Fig. 3(a) that adding an inductor in the loop radiator mainly has influence on the frequencies of the upper band.

The surface-current distributions at 2445 and 5780 MHz for the proposed loop and the upper portion of the large system ground are given in Fig. 7. First, the surface currents are seen mostly populated on the loop radiator and its small ground on the substrate. No current nulls are seen on the loop radiator at 2445 MHz, which indicates that the quarter-wavelength loop resonance is excited in the lower band. For the antenna excited at 5780 MHz, one current null denoted by a cross can be spotted along the resonant path on the L-shaped loop. This suggests that the upper-band resonance for the loop is of a half-wavelength loop mode. Second, on the small antenna ground are also distributed

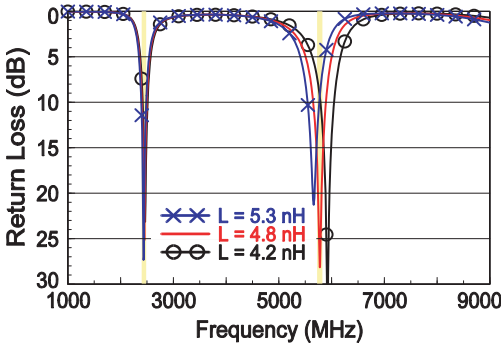

Figure 6. Simulated return loss for the loop antenna studied in Fig. 5 as a function of the inductor L.

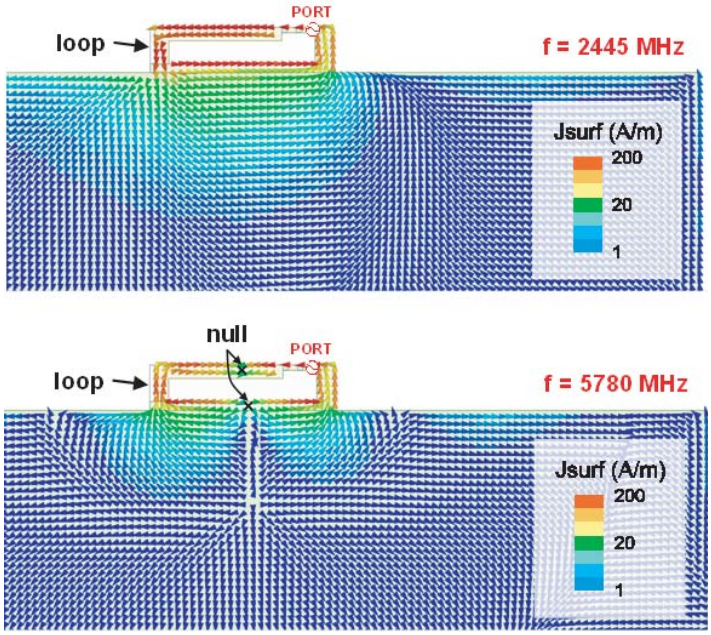

Figure 7. Simulated surface currents in the form of vectors excited at 2445 and 5780 MHz for the antenna studied in Fig. 5.

large surface image currents opposite those on the loop radiator. The L-shaped, loop structure is a half-wavelength loop radiator while that in combination with the image currents on the antenna ground exhibit a one-wavelength loop mode [22].

3. EXPERIMENTAL RESULTS

Figure 8 shows the measured and simulated return losses of a design prototype. The shaded frequency ranges mark the 2.4- and 5.8-GHz WLAN bands. The experimental data agree well with the simulation results. The two resonant modes for the lower and the upper bands are excited respectively. The impedance matching therein all exceeds the 9.6-dB return loss (about VSWR of 2), which is practically accepted for WLAN applications.

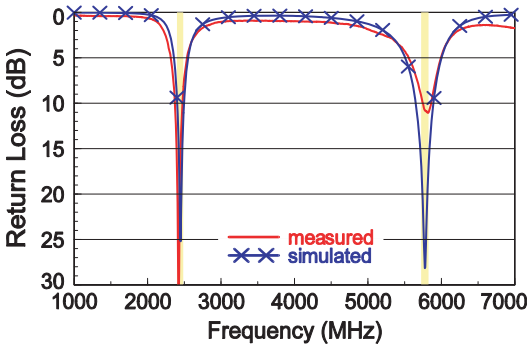

Figure 8. Measured and simulated return loss for the proposed antenna; $C = 0.1$ pF, $L = 4.8$ nH.

The over-the-air (OTA) performance of the antenna in free space was also studied. The measurement was taken at the $4\,\text{m} \times 4\,\text{m} \times 4\,\text{m}$, SATIMO chamber, which uses the conical-cut method, of model SG 64 [32]. Fig. 9 shows the measured, far-field radiation patterns for the prototype at 2442 and 5775 MHz, the center frequencies of the 2.4 and 5.8 GHz bands, in E_θ and E_ϕ fields. The patterns were normalized with respect to the peak gain in each cut. First, the omnidirectional radiation patterns are observed in the x-y planes over the two operating bands with larger radiation in the upper half space toward the $+z$ direction above the large system ground, similar to the radiation characteristics of the WLAN notebook computer antennas reported in [1–9]. Second, because the loop and its ground also form a close, one-wavelength loop structure at 5780 MHz as discussed in Fig. 7, the field strength

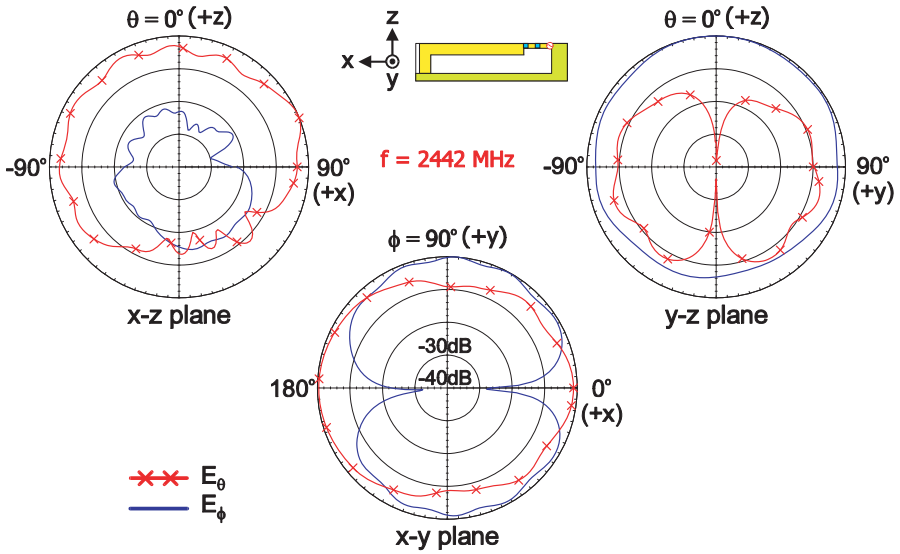

(a)

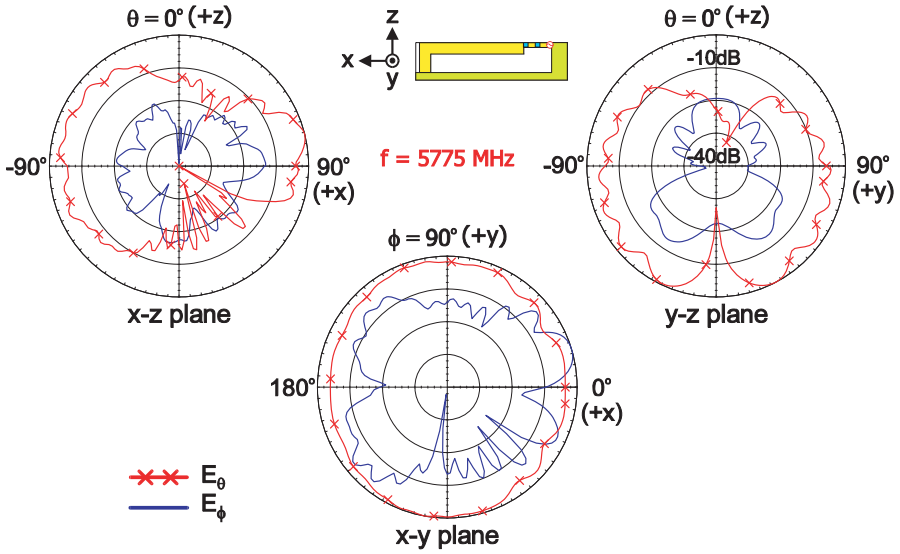

(b)

Figure 9. Measured radiation patterns of the proposed antenna at (a) 2442 MHz and (b) 5775 MHz.

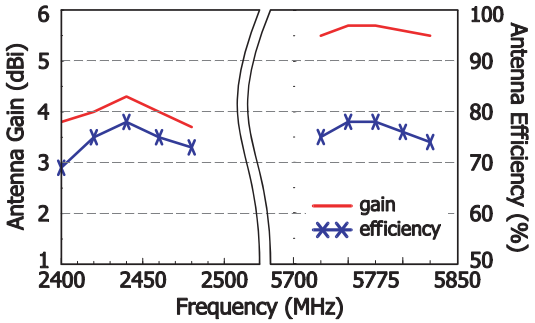

Figure 10. Measured peak antenna gain and antenna efficiency for the antenna studied in Fig. 9.

along the $\pm y$ axial directions are larger than that in the directions of $+x$ axis and $-x$ axis in the upper band. The measured, peak antenna gain and antenna efficiency against frequency are shown in Fig. 10. For 2.4 GHz operation, the peak antenna gain is the range of 3.7 to 4.3 dBi with antenna efficiency of 69–78%. Over the 5.8 GHz band, the gain is about 5.6 dBi with antenna efficiency of 74–78%. The OTA measurement here took account of antenna mismatch loss; the realized gain [33] and the antenna efficiency [34] were measured.

4. CONCLUSION

A new, printed loop antenna with a compact size of 5 mm × 20 mm, including the loop radiator and the small antenna ground, for dual-band WLAN operation has been presented. The loop structure was very simple and occupied an area of 4 mm × 13.8 mm. The quarter-wavelength loop mode was generated with the aid of the matching capacitor loaded between the antenna feed port and the loop radiator to cover the 2.4 GHz band. In addition, the operating frequencies of the half-wavelength loop mode can be adjusted for 5.8-GHz operation by tuning the values of the inductor in series with the capacitor. The results showed that the omnidirectional radiation patterns with antenna radiation efficiency larger than 70% over the lower and the upper bands were obtained. Owing to its small size and a low profile of 5 mm, the design can find some practical applications in the current narrow-bezel notebook computers and for future Gbps communications with multiple antennas integrated.

REFERENCES

1. Flint, E. B., B. P. Gaucher, and D. Liu, "Integrated antenna for laptop applications," U.S. Patent 6 339 400 B1, Jan. 15, 2002.
2. Liu, D. and B. Gaucher, "A triband antenna for WLAN applications," *IEEE Symposium on Antennas and Propagat.*, 18–21, Columbus, OH, 2003.
3. Hosoe, T. and K. Ito, "Dual-band planar inverted F antenna for laptop computers," *IEEE Symposium on Antennas and Propagat.*, 87–90, Columbus, OH, 2003.
4. Su, C. M., W. S. Chen, Y. T. Cheng, and K. L. Wong, "Shorted T-shaped monopole antenna for 2.4/5 GHz WLAN operation," *Microwave Opt. Technol. Lett.*, Vol. 41, 202–203, 2004.
5. Liu, D. and B. Gaucher, "A branched inverted-F antenna for dual band WLAN applications," *IEEE Symposium on Antennas and Propagat.*, 2623–2626, Monterey, CA, 2004.
6. Wong, K. L., L. C. Chou, and C. M. Su, "Dual-band flat-plate antenna with a shorted parasitic element for laptop applications," *IEEE Trans. Antennas Propagat.*, Vol. 53, 539–543, 2005.
7. Liu, H. W., S. Y. Lin, and C. F. Yang, "Compact inverted-F antenna with meander shorting strip for laptop computer WLAN applications," *IEEE Antennas Wireless Propagat. Lett.*, Vol. 10, 540–543, 2011.
8. Lee, C. T. and S. W. Su, "Tri-band, stand-alone, PIFA with parasitic, inverted-L plate and vertical ground wall for WLAN applications," *Microwave Opt. Technol. Lett.*, Vol. 53, 1797–1803, 2011.
9. Su, S. W., "Very-low-profile, 2.4/5-GHz WLAN monopole antenna for large screen-to-body-ratio notebook computers," *Microwave Opt. Technol. Lett.*, Vol. 60, 1313–1318, 2018.
10. Yeo, J., Y. J. Lee, and R. Mittra, "A novel dual-band WLAN antenna for notebook platforms," *IEEE Symposium on Antennas and Propagat.*, 1439–1442, Monterey, CA, 2004.
11. Chou, L. C. and K. L. Wong, "Uni-planar dual-band monopole antenna for 2.4/5 GHz WLAN operation in the laptop computer," *IEEE Trans. Antennas Propagat.*, Vol. 55, 3739–3741, 2007.
12. Lee, C. T. and K. L. Wong, "Uniplanar printed coupled-fed PIFA with a band-notching slit for WLAN/WiMAX operation in the laptop computer," *IEEE Trans. Antennas Propagat.*, Vol. 57, 1252–1258, 2009.
13. Liu, D. and B. Gaucher, "Performance analysis of inverted-F and slot antennas for WLAN applications," *IEEE Symposium on Antennas and Propagat.*, 14–17, Columbus, OH, 2003.
14. Su, C. M., H. T. Chen, F. S. Chang, and K. L. Wong, "Dual-band slot antenna for 2.4/5.2 GHz WLAN operation," *Microwave Opt. Technol. Lett.*, Vol. 35, 306–308, 2002.
15. Lee, C. T., S. W. Su, S. C. Chen, and C. S. Fu, "Low-cost, direct-fed slot antenna built in metal cover of notebook computer for 2.4-/5.2-/5.8-GHz WLAN operation," *IEEE Trans. Antennas Propagat.*, Vol. 65, 2677–2682, 2017.
16. Su, S. W., "Concurrent dual-band six-loop-antenna system with wide 3-dB beamwidth radiation for MIMO access points," *Microwave Opt. Technol. Lett.*, Vol. 52, 1253–1258, 2010.
17. Su, S. W., "High-gain dual-loop antennas for MIMO access points in the 2.4/5.2/5.8 GHz bands," *IEEE Trans. Antennas Propagat.*, Vol. 58, 2412–2419, 2010.
18. Hong, T. C. and S. W. Su, "Compact high-gain printed loop-antenna array integrated into a 5-GHz WLAN access point," *Microwave Opt. Technol. Lett.*, Vol. 52, 2261–2267, 2010.
19. Su, S. W. and T. C. Hong, "Printed, multi-loop-antenna system integrated into a concurrent, dual-WLAN-band access point," *Microwave Opt. Technol. Lett.*, Vol. 53, 317–322, 2011.
20. Su, S. W., "Printed loop antenna integrated into a compact, outdoor WLAN access point with dual-polarized radiation," *Progress In Electromagnetics Research C*, Vol. 19, 25–35, 2011.
21. Su, S. W. and C. T. Lee, "Low-cost dual-loop-antenna system for dual-WLAN-band access points," *IEEE Trans. Antennas Propagat.*, Vol. 59, 1652–1659, 2011.
22. Su, S. W., "Compact four-loop-antenna system for concurrent, 2.4- and 5-GHz WLAN operation," *Microwave Opt. Technol. Lett.*, Vol. 56, 208–215, 2014.
23. Morishita, H., Y. Kim, and K. Fujimoto, "Design concept of antennas for small mobile terminals and the future perspective," *IEEE Antennas Propagat. Mag.*, Vol. 44, 30–34, 2002.

24. Jung, B., H. Rhyu, Y. J. Lee, et al., "Internal folded loop antenna with tuning notched for GSM/GPS/DCS/PCS mobile handset applications," *Microwave Opt. Technol. Lett.*, Vol. 48, 1501–1504, 2006.
25. Wong, K. L. and C. H. Huang, "Printed loop antenna with a perpendicular feed for penta-band mobile phone application," *IEEE Trans. Antennas Propagat.*, Vol. 56, 2138–2141, 2008.
26. Chi, Y. W. and K. L. Wong, "Compact multi-band folded loop chip antenna for small-size mobile phone," *IEEE Trans. Antennas Propagat.*, Vol. 56, 3797–3803, 2008.
27. Chi, Y. W. and K. L. Wong, "Quarter-wavelength printed loop antenna with an internal printed matching circuit for GSM/DCS/PCS/UMTS operation in the mobile phone," *IEEE Trans. Antennas Propagat.*, Vol. 57, 2541–2547, 2009.
28. Wong, K. L. and Z. H. Feng, "On-frame dual-loop antenna with narrow ground clearance for the 2.4/5.2/5.8-GHz WLAN operation in the smartphone," *Microwave Opt. Technol. Lett.*, Vol. 58, 1480–1485, 2016.
29. Su, S. W., C. T. Lee, and S. C. Chen, "Compact, printed, tri-band loop antenna with capacitively-driven feed and end-loaded inductor for notebook computers," *IEEE Access*, Vol. 6, 6692–6699, 2018.
30. Pozar, D. M., *Microwave Engineering*, 3rd Edition, Chapter 3, 143–145, Wiley, New York, 2005.
31. ANSYS HFSS, ANSYS Inc., https://www.ansys.com/Products/Electronics/ ANSYS-HFSS.
32. SG 64, SATIMO, http://www.mvg-world.com/en/products/field_product_family/ antenna-measurement-2/sg-64.
33. Volakis, J. L., *Antenna Engineering Handbook*, 4th Edition, Chapter 6, 16–19, McGraw-Hill, New York, 2007.
34. Balanis, C. A., *Antenna Theory: Analysis and Design*, 3rd Edition, Chapter 2, Wiley, Hoboken, NJ, 2012.